ARMY RESEARCH LABORATORY

Method and Characterization of Pyroelectric Coefficients for Determining Material Figures of Merit for Infrared (IR) Detectors

by Mathew Ivill, Eric Ngo, and Melanie W. Cole

ARL-TR-6758 **December 2013**

NOTICES

Disclaimers

The findings in this report are not to be construed as an official Department of the Army position unless so designated by other authorized documents.

Citation of manufacturer's or trade names does not constitute an official endorsement or approval of the use thereof.

Destroy this report when it is no longer needed. Do not return it to the originator.

Army Research Laboratory
Aberdeen Proving Ground, MD 21005-5069

ARL-TR-6758 **December 2013**

Method and Characterization of Pyroelectric Coefficients for Determining Material Figures of Merit for Infrared (IR) Detectors

Mathew Ivill, Eric Ngo, and Melanie W. Cole
Weapons and Materials Research Directorate, ARL

REPORT DOCUMENTATION PAGE

Form Approved
OMB No. 0704-0188

1. REPORT DATE *(DD-MM-YYYY)*	2. REPORT TYPE	3. DATES COVERED (From - To)
December 2013	Final	NA

4. TITLE AND SUBTITLE
Method and Characterization of Pyroelectric Coefficients for Determining Material Figures of Merit for Infrared (IR) Detectors

5a. CONTRACT NUMBER

5b. GRANT NUMBER

5c. PROGRAM ELEMENT NUMBER

6. AUTHOR(S)
Mathew Ivill, Eric Ngo, and Melanie W. Cole

5d. PROJECT NUMBER

5e. TASK NUMBER

5f. WORK UNIT NUMBER

7. PERFORMING ORGANIZATION NAME(S) AND ADDRESS(ES)
U.S. Army Research Laboratory
ATTN: RDRL-WMM E
Aberdeen Proving Ground, MD 21005-5069

8. PERFORMING ORGANIZATION REPORT NUMBER
ARL-TR-6758

9. SPONSORING/MONITORING AGENCY NAME(S) AND ADDRESS(ES)

10. SPONSOR/MONITOR'S ACRONYM(S)

11. SPONSOR/MONITOR'S REPORT NUMBER(S)

12. DISTRIBUTION/AVAILABILITY STATEMENT
Approved for public release; distribution is unlimited.

13. SUPPLEMENTARY NOTES

14. ABSTRACT
This report describes the preliminary implementation of a characterization assembly to measure pyroelectric coefficients in order to evaluate the material figure of merit for pyroelectric infrared (IR) detector applications. The measurement uses a modified Byer-Roundy technique where pyroelectric currents are generated by periodically heating and cooling an electroded sample. Specifically, the sample temperature is modulated into a low frequency, small amplitude (a few degrees Celsius) triangular waveform while the resulting pyroelectric current is continuously monitored. The setup was designed around commercially available equipment and therefore does not necessarily require the addition of custom components. The pyroelectric currents from a thin 500 μm, single-crystal substrate of $LiTaO_3$ have been measured near 32 °C to verify the accuracy and internal consistency of the characterization assembly. An average value of -205 ± 6 ($\mu C/m^2K$) was measured for the $LiTaO_3$ using three electrode sizes and two temperature frequencies, which is close to the literature value of -176 ($\mu C/m^2K$).

15. SUBJECT TERMS
ferroelectric, pyroelectric, IR, infrared, sensor, detector, thermal, characterization

16. SECURITY CLASSIFICATION OF:			17. LIMITATION OF ABSTRACT	18. NUMBER OF PAGES	19a. NAME OF RESPONSIBLE PERSON
a. REPORT	b. ABSTRACT	c. THIS PAGE			Mathew Ivill
Unclassified	Unclassified	Unclassified	UU	20	19b. TELEPHONE NUMBER (*Include area code*) (410) 306-0766

Standard Form 298 (Rev. 8/98)
Prescribed by ANSI Std. Z39.18

Contents

List of Figures

1. Introduction

Infrared (IR) detectors have found wide-spread use in military applications including night-vision, rifle sights, surveillance gear, and tracking and guidance systems (*1*). These detectors provide a means for information collection and increased situational awareness, allowing for threat identification and informed decision making. The IR sensors used in these detectors can be categorized into two classes—Photon (or quantum) and Thermal—depending on the physics of operation. Photon detectors operate by the creation of an electrical signal in semiconducting material produced from the electronic absorption of incoming photons, and the signal is read as a photocurrent or at a photovoltaic p-n junction. These detectors can provide high-sensitivity and fast refresh rates and are typically found in applications with high-sensitivity requirements. Unfortunately, these detectors require sub-100 K cooling to lower thermal noise for optimal performance making them both bulky and expensive (*2*).

In contrast, thermal-type IR detectors rely on the measurement of a change in some physical property of a material in response to a change in temperature. The required change in temperature is induced by the impinging IR radiation and in many cases a highly efficient IR absorber is used to convert the incident radiation into thermal energy. Thermal detectors do not require cooling and are well suited for applications demanding detectors that are low cost, highly mobile (small and lightweight), and consume low power. This class includes a plethora of sensors, including those that respond by a resistive change (bolometers) or the thermal expansion of a material. One particularly useful class of thermal detector for IR imaging utilizes pyroelectric materials as sensing elements to generate a current in response to temperature changes. Pyroelectric-based detectors are frequently found in commercial products for motion sensing and fire (flame) detectors (*3*), and are currently used in military rifle sights and driver viewers and in the future may be implemented in enhanced night vision goggles and unattended ground imaging sensors (*2*).

The most critical component of the detector is the pyroelectric material used as the sensing element. Several material figure-of-merits (FoMs) have been developed as criteria for selecting the optimum materials for IR detector applications. The FoMs are directly related to the material pyroelectric coefficient, which in large part will determine the amount of signal generated by the material in response to a temperature change. Therefore, quantifiable determination of the pyroelectric coefficient is essential in order to optimize processing strategies for material development. This report describes a setup to easily evaluate the pyroelectric coefficient of thin pyroelectric capacitors. The setup uses forced, low-frequency and low-amplitude temperature oscillations to modulate a sample's temperature while the generated current is continuously monitored. The pyroelectric currents from a thin 500 μm, single-crystal substrate of $LiTaO_3$ have

been successfully measured near 32 °C to verify the accuracy and internal consistency of the characterization setup. Also, the basic pyroelectric effect, the material FoM for pyroelectric detectors, and methods to measure the material pyroelectric coefficient are briefly reviewed.

2. Pyroelectric Effect

Pyroelectricity is a property of polar dielectric materials and is described by a change in the spontaneous polarization of the material due to a change in temperature. Under constant electric field and stress, the polarization change is described by a vector—the pyroelectric coefficient—given by:

$$\boldsymbol{p} = \left(\frac{\partial \boldsymbol{D}}{\partial T}\right)_{\sigma,E} = \left(\frac{\partial \boldsymbol{P}}{\partial T}\right)_{\sigma,E} \tag{1}$$

where $\boldsymbol{D}$ is the dielectric displacement, $\boldsymbol{P}$ is the polarization, and σ and E denote, respectively, constant stress and constant electric field. Physically, the internal structure of the electric dipoles in the pyroelectric material are modified, such as the rotation or reorientation of molecular dipoles or a shift in the atomic arrangement of displacive-type ferroelectric crystals, during the temperature change. This causes a change in the spontaneous polarization and a subsequent change in the surface charge of the material. If a pyroelectric capacitor—formed by adding top and bottom electrodes to a pyroelectric material—is connected into an external circuit, the variation of surface charge will generate a current flow as charge is redistributed among the faces of the capacitor. This current is given by:

$$i_p = Ap\frac{dT}{dt} \tag{2}$$

where A is the effective area of the capacitor, p is the pyroelectric coefficient (in this case, the component of vector $\boldsymbol{p}$ perpendicular to the electroded surface), and $\frac{dT}{dt}$ is the time rate of change of temperature. Notice that if the temperature change is reversed, say from heating to cooling, the flow of current will also reverse. Thus, pyroelectricity is both a reversible effect and a dynamic effect—it only responds to *changes* in temperature. Once the temperature of the material becomes static, the polarization settles to equilibrium and ceases to generate additional current.

3. IR Detector Figure-of-Merits

From a materials perspective, it is important to develop criteria that can be used to assess (quantifiably) the performance of a material for a particular application based solely on material properties. Typically, material FoMs are developed that allow material assessment outside of

geometric and/or engineering constraints for the purpose of material selection. However, in the assessment of pyroelectric materials, there is not one global FoM that can be applied to all situations and the correct FoM must conform to the intended application of the material. This extends to the type of amplifier used at the output of the pyroelectric, the operation frequency of the detector, and the intended size of the pyroelectric element (*4*). Since pyroelectrics are essentially thermal transducers, both the electrical and thermal properties must be taken into account. Whatmore has reviewed the necessary analysis to derive the current and voltage response and subsequent FoMs for pyroelectric materials (*4*):

$$\textit{Current responsivity}\ \text{FoM}: F_i = \frac{p}{c'} \tag{3}$$

$$\textit{Voltage responsivity}\ \text{FoM}: F_v = \frac{p}{c'\epsilon\epsilon_o} \tag{4}$$

where c' is the volume specific heat, ϵ the material dielectric constant, and ϵ_o the permittivity of free space (8.85×10^{-12} F/m). Here the *current responsivity* (R_i) is defined as the amount of pyroelectric current generated per watt of incident radiation power on the pyroelectric element, $R_i = \frac{i_p}{W}$, where W is the incident power. Likewise, the *voltage responsivity* (R_v) is the amount of pyroelectric voltage produced per watt of incident power, $R_v = \frac{v_p}{W}$. The above FoMs can therefore be used to select materials that would endow the highest performance in regard to current or voltage response. The F_i merit is generally a sufficient choice for materials used at high frequency, such as in fast-pulse detectors, and F_v may be used as criteria for large area detectors with large element capacitance (*5*). The quality of a pyroelectric sensor, however, is not judged solely by the pyroelectric response but by the signal-to-noise ratio of the sensor, where the noise may be intrinsic or extrinsic in origin (*6*). The detector signal-to-noise performance is given by the specific detectivity, $D^* = \frac{A^{1/2} \cdot R_v}{\Delta V_N}$, where R_v represents the voltage responsivity, A the detector area, and ΔV_N the total electrical noise from all contributions in the detector circuit (*3*). The detection limit of a pyroelectric-based detector is typically limited by the Johnson noise (resistive noise) generated in the capacitor element. In this case, a useful FoM that weighs the material properties for optimal signal-to-noise ratio is given by (*3*):

$$\textit{Voltage responsivity}\ \text{FoM}: F_D = \frac{p}{c'\sqrt{\epsilon\epsilon_0 \tan\delta}} \tag{5}$$

where tan δ is the dielectric loss. The *Detectivity* FoM provides a convenient and often used metric to measure and compare a materials performance for thermal imaging applications. This can act as a selection criterion in order to optimize the fabrication and processing strategies of pyroelectric materials for IR imaging.

4. Pyroelectric Measurement

From the FoM perspective, a quantifiable value of the pyroelectric coefficient is essential in the evaluation of materials for IR detector applications. While commercially available equipment, such as LCR (inductance-capacitance-resistance) meters and impedance analyzers, are readily available to quantify the capacitance and dielectric loss, turn-key equipment specifically designed to measure pyroelectric coefficients are at the present time rather scarce. Instead, custom and home-built systems are usually assembled to characterize the pyroelectric properties using one of several quantifiable methods.

The methods for determining the pyroelectric coefficient can be divided into three categories—*static*, *indirect*, and *dynamic*—depending on the temperature stimulus and the parameter measured (*7*). *Static methods* are made at discrete temperatures and typically measure the amount of pyroelectric charge that is redistributed after an incremental change in temperature, so that the pyroelectric coefficient can be calculated from $p = \frac{1}{A\Delta T}\int Idt = \frac{1}{A}\frac{\Delta Q}{\Delta T} = \frac{1}{A}\frac{(Q_2-Q_1)}{(T_2-T_1)}$, where Q_2 and Q_1 are the amount of charge measured at temperatures T_2 and T_1 (*8*). *Indirect methods* measure the pyroelectric coefficient indirectly via measurement of another physical parameter—most commonly the polarization. For instance, a sample's remenant polarization is measured at incremental temperatures and the slope of the resulting data yields the pyroelectric coefficient from the relation $p = (\frac{dP}{dT})$. Typically, however, both the *static* and *indirect* methods are rarely used. *Static methods* are prone to charge compensation, either from leakage current through the sample or conduction through air and the *indirect methods* involving polarization may be prone to incomplete switching of the polarization or to fatigue (*6*).

It is the *dynamic methods* that are normally used to interrogate pyroelectric properties. These methods involve a continuous change in temperature and, most commonly, a concomitant measurement of the generated current. Measurements using linear ramps of constant $\frac{dT}{dt}$ are typically referred to as the Byer-Roundy technique (*9*). In this case, it can be difficult to distinguish and separate the *true* pyroelectric current from any superimposed drift or thermally stimulated currents not pyroelectric in origin. The measurement accuracy can be improved by periodically oscillating the temperature. Since the pyroelectric effect is a reversible process, the pyroelectric current generated from heating should be equal and opposite to that of cooling at the same rate. Oscillating the temperature allows separation of the *true* pyroelectric current response for improved accuracy.

A *dynamic* temperature waveform can be induced indirectly using the Chynoweth method (*10*), which uses chopped radiation from a laser or other light source to modulate the temperature of the sample and measure the resulting current. Typically, a lock-in amplifier is referenced to the frequency of a light chopper and measures the induced pyroelectric signal from the sample at the

chopper frequency. This method is advantageous since the measurement frequencies can closely match the operational frequency of a real thermal imaging device. However, the accurate assessment of the sample temperature can be difficult since it requires knowledge of the material heat capacity, surface emissivity, and the rate of heat transfer to and from the sample, making a quantifiable determination of the pyroelectric coefficient also difficult (*11*). Alternative methods can be used to modulate the sample temperature directly; for example, by using modern Peltier devices and thermoelectric modules. These measurements are taken at lower frequencies, typically by applying a small temperature waveform of less than 1 Hz. The resulting pyroelectric current signal is proportional to the derivative of the temperature waveform. In the case of a sinusoidally varying temperature, the pyroelectric current will be 90° out-of-phase with the temperature oscillation since it is proportional to the time derivative of the driven sine wave. Alternatively, if a triangular temperature function is used, the current response will be represented by a square wave with positive and negative valued crests that represent the pyroelectric current for the given temperature rate of change. The pyroelectric current is then evident from a graph of current versus time and can be compared (verified) to the timing of the temperature waveform. The resulting current can also be averaged over multiple cycles to obtain a more accurate value. This type of measurement has been discussed in several reports (*11*, *12*, *13*) and has been used, for instance, to measure pyroelectric properties of Pb-based relaxor-ferroelectric single crystals (*14*).

5. Preliminary Assembly and Verification of Characterization Setup

The setup described in this report uses the low-frequency temperature oscillation method described above, and is designed to measure the pyroelectric current from thin ferroelectric samples. The setup assembly is similar to those described in the literature (*11*) but mostly incorporates commercially-available hardware. The setup consist of three main components: (1) A temperature regulated thermoelectric stage; (2) A high-sensitivity electrometer; and (3) A computer running custom LabView programs for instrumentation control, timing, and data collection. The complete setup diagram can be seen in figure 1.

A commercially available thermoelectric temperature stage (TE Technology, Inc.) is used to regulate the temperature of the sample. The stage includes a bidirectional proportional-integral-derivative (PID) controlled temperature controller that provides pulse-width modulated output to the thermoelectric module (TE Technology, Inc. model TC-24-25R). Temperature feedback is monitored by a thermistor sensor clamped to the surface of the heating/cooling block of the stage. The temperature controller is connected to a computer desktop through an RS232 serial communication cable. This stage is integrated into the center of a probe station so that the top contact of the sample can be accessed with a micro-positioner probe and surrounded by a desiccator box. For the measurements presented here, the stage is grounded to the electrometer

so that the backside contact on the sample is grounded with respect to the top contact. Custom LabView drivers are used to send basic commands to operate the stage from the main LabView program structure. A Keithley 6517B electrometer is used to monitor the generated pyroelectric currents from the sample. Current values are fetched from the electrometer every few seconds through the LabView program and saved with the temperature and timing data. The internal electrometer settings are used to average data readings (a setting of 50 readings was used for the collection of the data in this report) and to subtract the initial offset current in the circuit before measurement.

Pyroelectric measurements have been made on a 500 µm thick, z-cut, single-crystal $LiTaO_3$ wafer that is polished on both faces of the wafer (obtained from MTI Corporation). The wafer was diced into a substrate near 2.5 cm × 3.5 cm in size and sequentially cleaned in sonicating baths of acetone (5 min) and isopropyl alcohol (5 min) and blown dry with N_2. The backside of the substrate was covered with a blanket layer of 150-nm-thick Pt film deposited by DC magnetron sputtering at room temperature. Top electrodes of 150-nm-thick Pt were then deposited through a stainless steel shadow mask with circular holes approximately 5 mm, 4 mm, and 3 mm in diameter. The top contacts were imaged under an optical microscope and each contact was measured using image analysis software to obtain the *actual* electrode areas for use in calculating the pyroelectric coefficient.

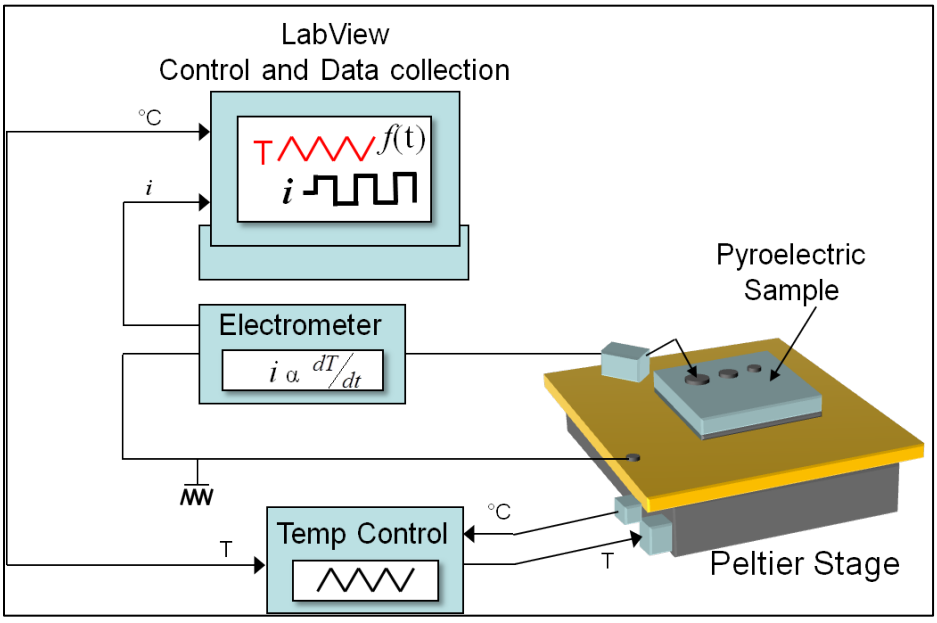

Figure 1. Pyroelectric instrumentation and setup.

Figure 2 shows a trial of the measurement on a nominally 3-mm-diameter contact (actual measured contact area of 9.0463 mm^2). The current switches predictably upon heating and cooling and has an average magnitude of 37.7 (pA). This leads to a calculated pyroelectric coefficient of –208.4 ($\mu C/m^2K$). This and additional measurements were conducted slightly above ambient temperature (T_o=32 °C) at frequencies of 2.5 mHz (and 5.0 mHz) over a temperature range of 4 °C. This equates to temperature rates of 0.02 °C/s (and 0.04 °C/s) for the ramp segments of the triangular cycle. The ramp is built digitally in LabView and digital set-points are sent in increments of 0.1 K—the resolution of the temperature controller—in specified time intervals based on the desired ramp rate. This rate was chosen because it provides an achievable balance between generating an adequate current signal (i_p proportional to $\frac{dT}{dt}$) while maintaining thermal equilibrium between the sample and heater stage with controlled rates. The temperature controller exhibited a small amount of overshoot at the inflection points of the triangular waveform and PID controls were selected that provided quick response back to the intended set-points after passing the inflection points. This resulted in an initial faster rate as the temperature catches up to the next several set-points, but quickly settles and continuously follows the programmed rate until the next inflection. As seen in figure 2, the faster ephemeral rates cause the pyroelectric current to increase and appear as peaks in the current waveform as the temperature inflections are passed. These peaks are easily accounted for and only the currents measured during the steady ramps are used for the analysis. These momentary overshoots could limit the minimal size of ΔT (or maximum achievable frequency), since at small ΔT the stage would never reach the steady temperature ramp of the programmed set-points. However, this assembly is anticipated to use low frequencies (several mHz) and ΔT of 1 °C to 4 °C, which are large enough to obtain accurate data. Additionally, the existing stage could be replaced by a smaller heating block connected to the thermoelectric module in order to lower the thermal mass and provide a quicker response.

Figure 3 shows the overall results of pyroelectric coefficient measurements conducted with the three contact areas and two temperature ramp rates. Measuring a similar value of pyroelectric coefficient over multiple contact areas and ramp rates ensures the system is measuring the desired parameter and not spurious signals. The inset of figure 3 shows a linear scaling behavior between contact size and pyroelectric current as anticipated. The average coefficient, over all trials, is –205 ± 6 ($\mu C/m^2K$), which represents the average value ± one standard deviation. This is in agreement with often quoted values of the pyroelectric coefficient given in the literature of –230 (*4*) and –176 (*15*). The value of course depends on the actual sample material measured and sample processing and quality will determine the overall pyroelectric properties. Therefore, the most important note is that of the internal consistency and correct scaling behavior of the measurements in figure 3, which show a reproducible value for the data set.

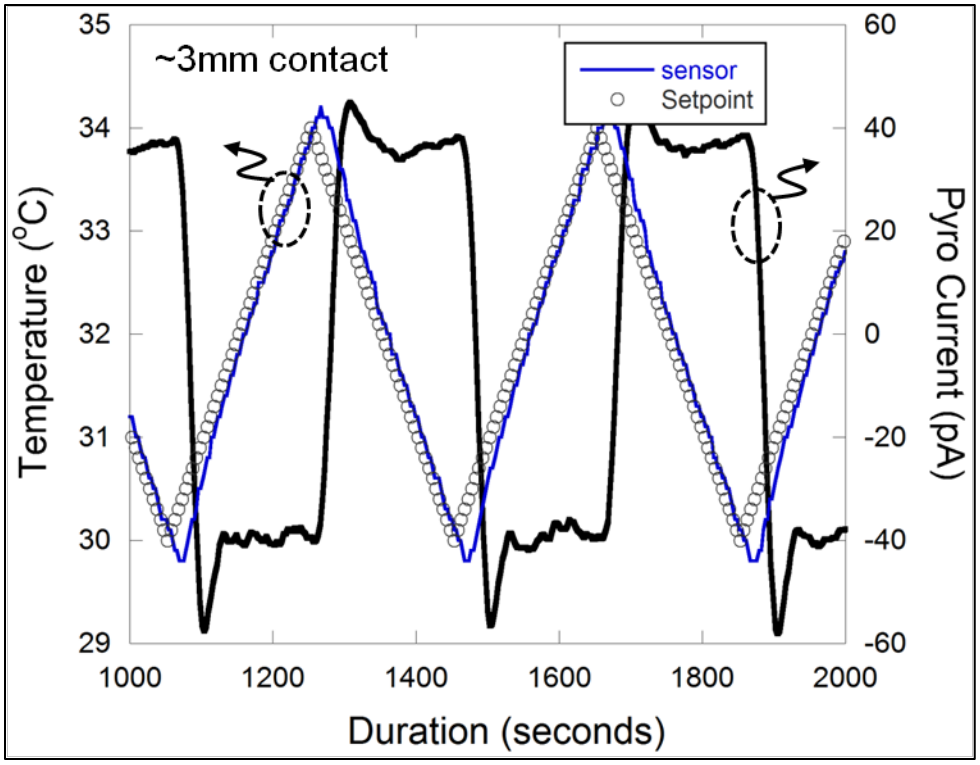

Figure 2. Pyroelectric measurement on $LiTaO_3$ with nominal 3-mm-diameter contact. The circular dots and blue line are the temperature (triangular-waveform) set-points and sensor readings, respectively. The black line is the resulting pyroelectric current (square-waveform) readings.

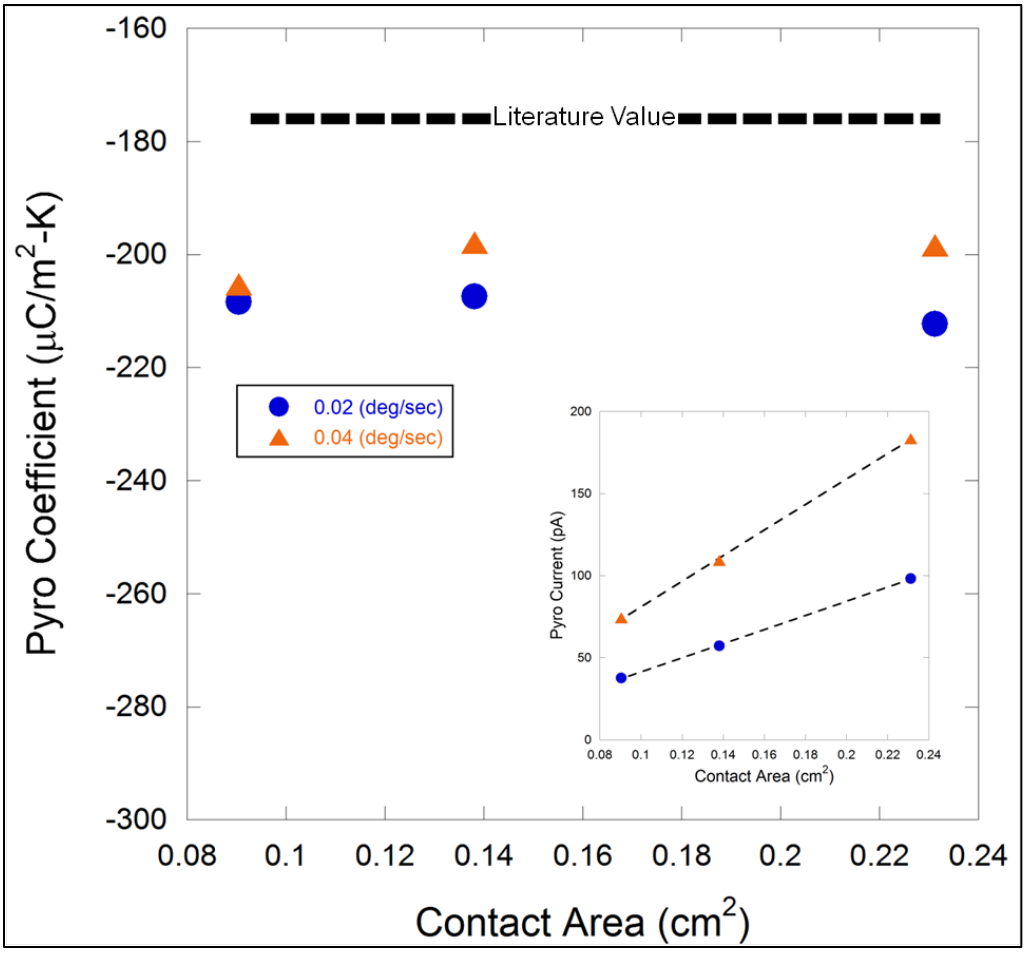

Figure 3. Pyroelectric results on $LiTaO_3$ with various contact size and temperature rates of change. Literature value of –176 ($\mu C/m^2K$) taken from reference 15. The inset shows the linear scaling of the measured pyroelectric current vs. contact area for each temperature rate.

If desired, digital filtering can also be applied to smooth the resulting data. An additional LabView program applies a user-adjustable, low-pass Butterworth filter after data collection to smooth the square-wave current data. A comparison between collected and filtered data for measurements on a nominal 4-mm-diameter contact is given in figure 4. However, all other data reported here uses the collected (unfiltered) data to extract the pyroelectric currents.

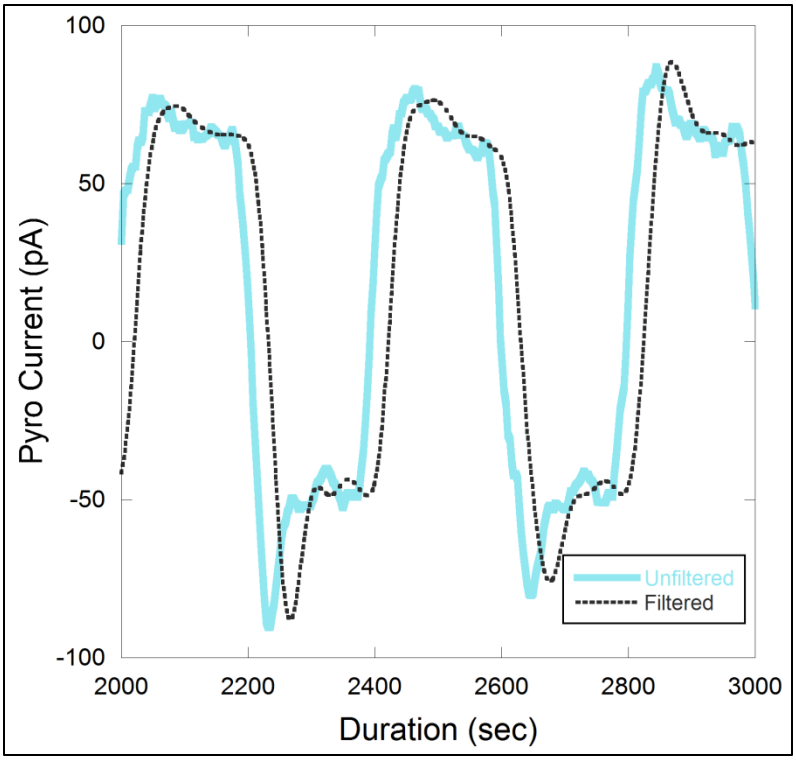

Figure 4. Comparison between collected (unfiltered) pyroelectric data (solid line) and the same data digitally filtered using a low-pass Butterworth filter in LabView (dotted line).

6. Conclusions

The pyroelectric coefficient is an essential material property used for evaluating the performance of materials for pyroelectric-based IR detectors. Indeed, several FoM—all of which rely on the pyroelectric coefficient—have been established as a materials selection criterion for these detectors. The preliminary assembly of a setup to evaluate pyroelectric coefficients of ferroelectric samples was described and tested using a thin substrate of $LiTaO_3$. The setup uses a modified Byer-Roundy method to continuously monitor the pyroelectric current from a sample during forced temperature oscillations. Measured pyroelectric currents, on the order of 10 to 100 pA, from the $LiTaO_3$ correctly modulate/switch in accordance with the forced temperature waveform and scale correctly (linearly) with electrode area. An average pyroelectric coefficient of –205 ($\mu C/m^2K$) was successfully measured over multiple trials, which is near the literature value of $LiTaO_3$. More importantly, the setup shows internal consistency between measurements. The current implementation is restricted to low frequencies, less than 10 mHz, for temperature oscillations due to poorer temperature control at higher frequencies. Modifications and improvements to the overall setup will continue to be made as more samples are evaluated and

the measurement accuracy and error will be further evaluated with additional trials. A similar setup is being constructed, as described previously (*16*), that uses a waveform generator and temperature controller to regulate a thermoelectric module and a lock-in amplifier to monitor the pyroelectric-induced current.

7. References

1. Tidrow, M. Z. Device Physics and State-of-the-Art of Quantum Well Infrared Photodetectors and Arrays. *Materials Science and Engineering B* **2000**, *74*, 45–51.
2. Nothwang, W. D.; Cole, M. W.; Goldberg, A. Cutting Edge Infrared Detector Materials Enhance Army's Night Vision and Targeting Capabilities. *AMPTIAC Quarterly* **2004**, *8* (4), 111–117.
3. Whatmore, R. W. Pyroelectric Arrays: Ceramics and Thin Films. *J. Electroceramics* **2004**, 13, 139–147.
4. Whatmore, R. W. Pyroelectric Devices and Materials. *Rep. Prog. Phys.* **1986**, *49*, 1335–1386.
5. Lee, M. H.; Guo, R.; Bhalla, A. S. Pyroelectric Sensors. *J. Electroceramics* **1998**, *2* (4), 229–242.
6. Muralt, P. Micromachined Infrared Detectors Based on Pyroelectric Thin Films. *Rep. Prog. Phys.* **2001**, *64*, 1339–1388.
7. Lang, S. B. *Source Book of Pyroelectricity*; Gordon and Breach, Science Publishers, Inc.: New York, NY, 1974.
8. K-C, K. *Dielectric Phenomena in Solids*; Elsevier Academic Press: London, England, 2004, p 272.
9. Byer, R. L.; Roundy, C. B. Pyroelectric Coefficient Direct Measurement Technique and Application to a nsec Response Time Detector. *Ferroelectrics* **1972**, *3*, 333–338.
10. Chynoweth, A. G. Dynamic Method for Measuring the Pyroelectric Effect With Special Reference to Barium Titanate. *J. Applied Physics* **1956**, *27*, 78–84.
11. Daglish, M. A Dynamic Method for Determining the Pyroelectric Response of Thin Films. *Integrated Ferroelectrics* **1998**, *22*, 473–488.
12. Dias, C.; Simon, M.; Quad, R.; Das-Gupta, D. K. Measurement of the Pyroelectric Coefficient in Composites Using a Temperature-Modulated Excitation. *J. Phys. D: Appl. Phys.* **1993**, *26*, 106–110.
13. Hartley, N. P.; Squire, P. T.; Putley, E. H. A New Method of Measuring Pyroelectric Coefficients. *J. Physics E: Scientific Instruments* **1972**, *5*, 787–789.

14. Davis, M.; Damjanovic, D.; Setter, N. Pyroelectric Properties of (1-x)Pb($Mg_{1/3}Nb_{2/3}$)O_3-x$PbTiO_3$ and (1-x)Pb($Zn_{1/3}Nb_{2/3}$)O_3-x$PbTiO_3$ Single Crystals Measured Using a Dynamic Method. *J. Applied Physics* **2004**, *96* (5), 2811–2815.

15. Lang, S. B. Pyroelectricity: From Ancient Curiosity to Modern Imaging Tool. *Physics Today* **2005**, *58* (8), 31–36.

16. Sarney, W. L.; Little, J. W.; Livingston, F. E.; Cole, M. W.; Niesz, K.; Ould-Ely, T.; Morse, D. E. *Bio-Inspired Materials Research for Improved Sensitivity Low-Cost Uncooled Infrared (IR) Detector Focal-Plane Arrays*; ARL-TR-5172; U.S. Army Research Laboratory: Aberdeen Proving Ground, MD, April 2010.

NO. OF COPIES	ORGANIZATION
1 (PDF)	DEFENSE TECHNICAL INFORMATION CTR DTIC OCA
1 (PDF)	DIRECTOR US ARMY RESEARCH LAB IMAL HRA
1 (PDF)	DIRECTOR US ARMY RESEARCH LAB RDRL CIO LL
1 (PDF)	GOVT PRINTG OFC A MALHOTRA

ABERDEEN PROVING GROUND

15 (5 PDF, 10 HC)	DIR USARL RDRL WMM E M IVILL (10 HC) E H NGO M W COLE J P SINGH C BRENNAN